Microwave and Millimeter Wave Forward Modeling Results from the 2004 North Slope of Alaska Arctic Winter Radiometric Experiment

E. R. Westwater[1], D. Cimini[1], V. Mattioli[2] , M. Klein[1], V. Leuski[1], A. J. Gasiewski[3], S. Dowlatshahi[4], J. S. Liljegren[5] , B. M. Lesht[5] and J. A. Shaw[6]
[1]Cooperative Institute for Research in Environmental Sciences, University of Colorado/NOAA-Environmental Technology Laboratory, 325 Broadway, Boulder, CO 80305, USA
[2]Dipartimento di Ingegneria Elettronica e dell'Informazione, Università di Perugia via G. Duranti 93, 06125 Perugia, Italy
[3]NOAA-Environmental Technology Laboratory, 325 Broadway, Boulder, CO 80305, USA
[4]Science and Technology Corporation**,** 325 Broadway, Boulder, CO 80305, USA
[5]DOE/Argonne National Laboratory, Bldg 203, 9700 South Cass Avenue, Argonne, IL 60439, USA
[6]Department of Electrical and Computer Engineering, Montana State University, 610 Cobleigh Hall, Bozeman, MT 59717, USA

Introduction

The 2004 Arctic Winter Radiometric Experiment was conducted at the North Slope of Alaska (NSA) Atmospheric Radiation Measurement's (Program) (ARM) field site near Barrow, Alaska from March 9 to April 9, 2004. The goals of the experiment were: to study the microwave and millimeter wave radiometric response to water vapor and clouds during cold and dry conditions; to obtain data for forward model studies at frequencies ranging from 22.235 to 400 GHz, to demonstrate new Environmental Technology Laboratory's (ETL) radiometric receiver and calibration technology and to compare both radiometric and in situ measurements of water vapor. A description of the experiment and preliminary data is given by Westwater et al. (2004), a complete description of ETL's Ground-based Scanning Radiometer (GSR) is given in this Proceedings by Cimini et al. (2005), and a comparison of in situ radiosonde data with data from the dual-channel ARM Microwave Radiometer and the 12-channel ARM Microwave Radiometer Profiler (MWRP) is given in this Proceedings by Mattioli et al. (2005). Another paper describing initial results from this experiment is given by Dowlatshahi et al. (2005). In this paper, as a necessary step in improving water vapor measurements at low concentrations, we give our results of clear sky forward model comparisons for radiometric channels near the 183.31 GHz water vapor line. Table 1 summarizes the instruments used the studies of this paper. We also present examples of data from an Infrared Cloud Imager (Thurairajah and Shaw, 2005) that, in addition to its application to cloud research, has the potential for studying the effects of clouds within a radiometer's beam.

Clear Air Forward Model Studies Based on Vaisala RS-90 and Chilled Mirror Radiosondes

As discussed by Mattioli et al. (2005), Vaisala RS90 radiosondes were launched 4 times per day from the ARM Duplex (Dplx), once per day from the location of all of the ARM

instruments, the so called “Great White” (GW), and eight Chilled Mirror “Snow White” radiosondes were launched from the Duplex on the same balloons that also carried the Vaisala RS90 humidity sensor. In addition to these data, we also acquired synoptic soundings from the NOAA/National Weather Service (NWS) launches within the city of Barrow. The Mattioli et al. (2005) paper also contains a more complete discussion of each of the humidity sensors used on the radiosonde launches. Because of substantial differences between NWS and Vaisala radiosondes, and because we suspect that the NWS upper level humidity data are incorrect, our statistical analysis here does not include the NWS radiosondes. However, to give an idea of the differences that may arise between simultaneous radiosondes, we show one of our typical comparisons in Figure 1. It is seen that significant differences in RH exist, especially above 6-8 km. A complete analysis of radiosonde statistics for this experiment is given by Mattioli et al., (2005).

Our basic forward model studies involve comparing calibrated brightness temperatures T_B from measurements of the GSR (see Cimini et al., 2005) with T_B calculated from radiosondes using five clear-air absorption models: (1) Liebe and Layton (1987)-LBE87, (2) Liebe et al., 1993- LBE93, Rosenkranz (1998, 1999)- ROS98, Rosenkranz (2003)-ROS03, and Liljegren et al., (2005)-LIL05. An example of calculations for the Chilled Mirror radiosonde from Figure 1 is shown in Figure 2. In the right figure, we see that around the 183.31 GHz line, differences can be as large as about 15 K.

The T_B calculations shown in Figure 2 are monochromatic. To compare such calculations with measurements, the frequency response characteristics of each channel must be taken into account. For the GSR channels near 183.31 GHz, a double sideband bandpass must be used. Two representative bandpass filter functions, as supplied by the manufacturer, are shown in Figure 3. For each of our T_B estimates, about 1000 monochromatic calculations were averaged to yield the double-sided average.

To compare measured GSR data with the model calculations, we first removed outliers from the radiometric data by applying a 9-point median filter to the raw data, and identified cloudy conditions by use of the MWRP infrared (IR) channel. For subsequent comparisons with radiosondes, 10 min averages of the data were constructed. Only data with the IR clear sky threshold of $T_B = 223.2$ K were used. An example of our data for Julian day 73 (March 13, 2004) is shown in Figure 4.

We have made detailed statistical comparison between all five models and all of the available radiosonde types and locations; we show in Table 2 only the results of calculations based on RS90 radiosonde data taken at the Duplex using LBE87,LBE93,ROS98, ROS03 and LIL05. We note that there is a maximum bias of less than 1.8 K for LIL05 and 3.5 K for ROS03. In terms of bias, ROS03 is generally slightly better than LIL05. The maximum rms difference for LIL05 is about 4 K and about 5 K for ROS03. ROS98/ROS03/LIL05 seem to agree very well for the three opaque channels (within 1K), while LBE87/93 show alternatively large biases (all values from 1 to 6 K). For more transparent channels, LBE93 is substantially at variance with the measurements. In contrast, LIL05 stays within 1.8 K, which would support the choice of the MT_CKD continuum; conversely, LBE87 doesn't behave badly either (within 2.2K).

It should be clearly understood that these rms values reflect not only model differences but also calibration and radiosonde errors. Of the latter two error sources, we believe that radiosonde errors are the most important.

In Figure 5 (and in the remainder of this paper) we will only show detailed comparisons with LIL05. We note that the biases are generally of the order of 1-3 K with a range of variation in T_B of some 100 to 150 K. An exception is for the 183.31 ± 4.7 GHz, which, for the Great White, has a bias of almost 7 K. In addition, for a given model, there is a considerable variation of all of the statistical parameters between each of the three radiosonde types or location. Since roughly 75% of the Duplex radiosondes were not taken simultaneously with those of the Great White, we extracted from the Duplex radiosondes those taken within 20 min of Great White. The results of these comparisons are shown in Figure 6. We note that there is still a large bias at 183.31 ± 4.7 GHz, but the differences between the two radiosonde calculations are much smaller, being of the order of 1 to 1.5 K. Mattioli et al. (2005) shows that the Precipitable Water Vapor difference between the simultaneous radiosondes (daytime only) at the two locations was 0.005 cm.

Infrared Cloud Imager Observations

As part of this experiment we deployed the Infrared Cloud Imager (ICI), a thermal infrared sensor that measures spatial cloud statistics from downwelling atmospheric radiance in the 8-14 μm spectral band (Thurairajah and Shaw 2005). Figure 7 shows two example ICI images recorded during March 2005 at the NSA site, indicating the cold equivalent brightness temperature of the clouds and clear sky. At NSA the sky tends to be significantly cloudy or clear, with short transition periods of broken cloudiness. The ICI images are used to identify clear and cloudy periods, to identify brief sporadic clouds, and to investigate the variation of microwave and mm-wave radiometer signals as a function of cloudiness within the radiometers' fields of view.

Conclusions

For clear air conditions, we have compared calibrated GSR measurements near 183.31 GHz with RTE calculations based on five absorption models. Of the five, the models of Liljegren et al. (2005) and Rosenkranz (2 003) appear to be the most accurate over all of the channels. With this model, comparisons with measurements were generally with 3-4 K rms. As shown by comparisons with two simultaneous radiosondes, it appears that radiosonde errors still form a considerable portion of this error. However, because of the high sensitivity of these measurements to water vapor, a relative accuracy of about 2-3 % is expected. This accuracy of GSR and forward models will substantially improve measurements of water vapor at low concentrations.

Future plans

- Conduct forward model studies at other channels
- Derive meteorological products from GSR data
- Use combined active-passive retrieval of meteorological products
- Use ICI image data to investigate the effect of variable clouds within the mm-wave radiometer field of view
- Determine the information content of angular scan data

References

Cimini, D., A. J. Gasiewski, M. Klein, E. R. Westwater, V. Leuski,and S. Dowlatshahi, "Ground-based Scanning Radiometer Measurements during the Water Vapor IOP 2004: a valuable new data set for the study of the Arctic atmosphere". Proc. of the 15th. ARM Science Team Meeting, Daytona Beach, FL, March 14-18 2005.

Dowlatshahi, S.G., A.J. Gasiewski, T. Uttal, M. Klein, E.R. Westwater and D. Cimini, "Detection of Arctic Cloud Ice Properties Using Submillimeter-wave Radiometers," Proc. of the 8th Conference on Polar Meteorology and Oceanography, 85th AMS Annual Meeting, January 9-13, 2005.

Liebe, H. J. and D.H. Layton, "Millimeter Wave Properties Of The Atmosphere: Laboratory Studies And Propagation Modeling," National Telecommunications and Information Administration (NTIA) Report 87-24, 1987, 74 pp. (available from the National Technical Information Service, 5285 Port Royal Road, Springfield, VA, 22161).

Liebe, H. J, G.A. Hufford, and M.G. Cotton, "Propagation modeling of moist air and suspended water/ice particles at frequencies below 1000 GHz," *AGARD conference proceedings* 542, 3.1–3.10, 1993.

Liljegren, J. C., S. A. Boukabara, K. Cady-Pereiria, and S. A. Clough, "The Effect of the Half-Width of the 22-GHz Water Vapor Line on Retrievals of Temperature and Water Vapor Profiles with a Twelve-Channel Microwave Radiometer," *IEEE Transactions on Geoscience and Remote* Sensing, **43(5)**, 1102-1108, 2005.

Mattioli, V., E. R. Westwater, D. Cimini, J. S. Liljegren, B. M. Lesht, S. Gutman, and F. Schmidlin, "Analysis of Radiosonde and PWV data from the 2004 North Slope of Alaska Arctic Winter Radiometric Experiment," Proc. of the 15th. ARM Science Team Meeting, Daytona Beach, FL, March 14-18 2005.

Rosenkranz, P.W., "Water vapor microwave continuum absorption: a comparison of measurements and models", *Radio Sci*., **33**, 919-928, 1998.

Rosenkranz, P. W., Correction to "Water vapor microwave continuum absorption: a comparison of measurements and models," *Radio Sci.*, **34(4)**, 1025, 1999.

Rosenkranz, P. W., Private communication.

Thurairajah, B. and J. A. Shaw, 2005, "Cloud Statistics Measured with the Infrared Cloud Imager," *IEEE Trans. Geosci. Rem. Sens.* (in press).

Westwater, E.R., Klein, M., Gasiewski, A., Leuski, V., Shaw, J.A., Mattioli, V., Cimini, D., Liljegren, J.C., Lesht, B.M., Zak, B.D., Uttal, T., Hazen, D.A., Weber, B.L., and Dowlatshahi, S., 2004, "The 2004 North Slope of Alaska Arctic Winter Radiometric Experiment." *Proc. of 14th ARM Science Team Meeting*. March 22-26, 2004, Albuquerque, New Mexico. [Available on-line at: http://www.arm.gov/publications/proceedings/conf14/extended_abs/westwater-er.pdf].

Table 1.The subset of instruments deployed during the NSA 2004 Arctic Winter Radiometric Experiment whose data are shown here. T-temperature. ρ_V-water vapor density. RH-relative humidity. P-pressure. Z-altitude. CBT-cloud base temperature.

INSTRUMENT	**FREQUENCY(GHz)**	**PARAMETER**
ETL GSR	**183.31 (±0.5,±1,±3,±5, ±7,±12,±16)**	**PWV, ρ_V (z)**
MSU ICI	**8-14 μm**	**Cloud Images, statistics**
ARM MWRP	**10 μm**	**CBT**
RADIOSONDE	**LAUNCH FREQUENCY**	**PARAMETER**
ARM Dplx	**4 per day**	**T(z), RH(z), P(z)**
ARM GW	**1 per day**	**T(z), RH(z), P(z)**
NASA SW	**8 total**	**T(z), RH(z), P(z)**

Table 2. Comparison of GSR measurements with five forward models calculated from Vaisala RS90 radiosondes (N=83) that were launched at the ARM Duplex. The model with the smallest bias is highlighted in red.

Frequency - 183.31 GHz	MODEL	BIAS(K) calc-meas	STD(K)	SLOPE β Calc=α +β meas	INTERCEPT α (K)
± 0.55	LBE87	-3.76	3.98	1.12	-30.70
	LBE93	-0.34	2.26	1.03	-8.19
	ROS98	-0.59	2.37	1.04	-10.29
	ROS03	-1.03	2.49	1.05	-12.76
	LIL05	-0.80	2.39	1.04	-11.08
± 1	LBE87	-2.39	3.27	1.07	-18.60
	LBE93	1.28	2.24	1.00	0.87
	ROS98	0.27	2.35	1.02	-4.79
	ROS03	-0.03	2.36	1.03	-5.90
	LIL05	0.26	2.30	1.02	-4.22
± 3	LBE87	1.19	3.55	1.04	-5.56
	LBE93	6.08	3.43	1.01	4.19
	ROS98	-1.09	3.76	1.04	-9.05
	ROS03	-0.10	3.53	1.04	-6.64
	LIL05	0.85	3.43	1.03	-4.80
± 4.7	LBE87	-0.23	3.87	1.04	-6.45
	LBE93	5.46	3.94	1.04	-0.11
	ROS98	-5.16	3.72	1.04	-10.30
	ROS03	-3.43	3.56	1.03	-7.83
	LIL05	-1.78	3.54	1.03	-6.13
± 7	LBE87	2.20	4.02	1.06	-3.78
	LBE93	8.77	4.87	1.08	0.47
	ROS98	-3.18	3.16	1.02	-5.60
	ROS03	-1.15	3.15	1.02	-3.50
	LIL05	1.28	3.35	1.03	-2.11
± 12	LBE87	-0.04	3.52	1.10	-6.46
	LBE93	7.62	5.74	1.18	-4.23
	ROS98	-3.49	2.35	1.04	-6.26
	ROS03	-1.60	2.37	1.04	-4.48
	LIL05	1.66	3.14	1.08	-3.74
± 16	LBE87	-1.89	2.51	1.07	-5.90
	LBE93	6.18	5.06	1.20	-4.43
	ROS98	-4.21	1.82	1.02	-5.37
	ROS03	-2.49	1.83	1.02	-3.68
	LIL05	1.06	2.56	1.08	-3.24

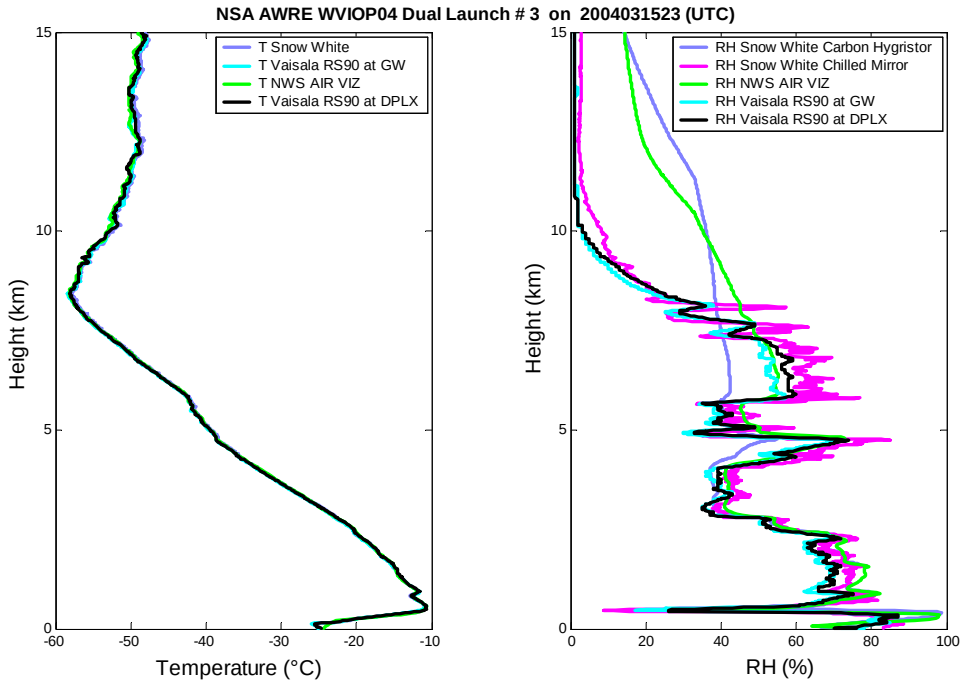

Figure 1. Comparison of Temperature and Relative Humidity measurements from 5 simultaneous radiosonde launches near Barrow, AK, on March 15, 2004, 2300 UTC. The NWS AIR VIZ and the Snow White Carbon Hygristor measure Relative Humidity by means of resistors; The Vaisala RS90 uses capacitative measurements of Relative Humidity, and the Chilled Mirror measures frost point temperature.

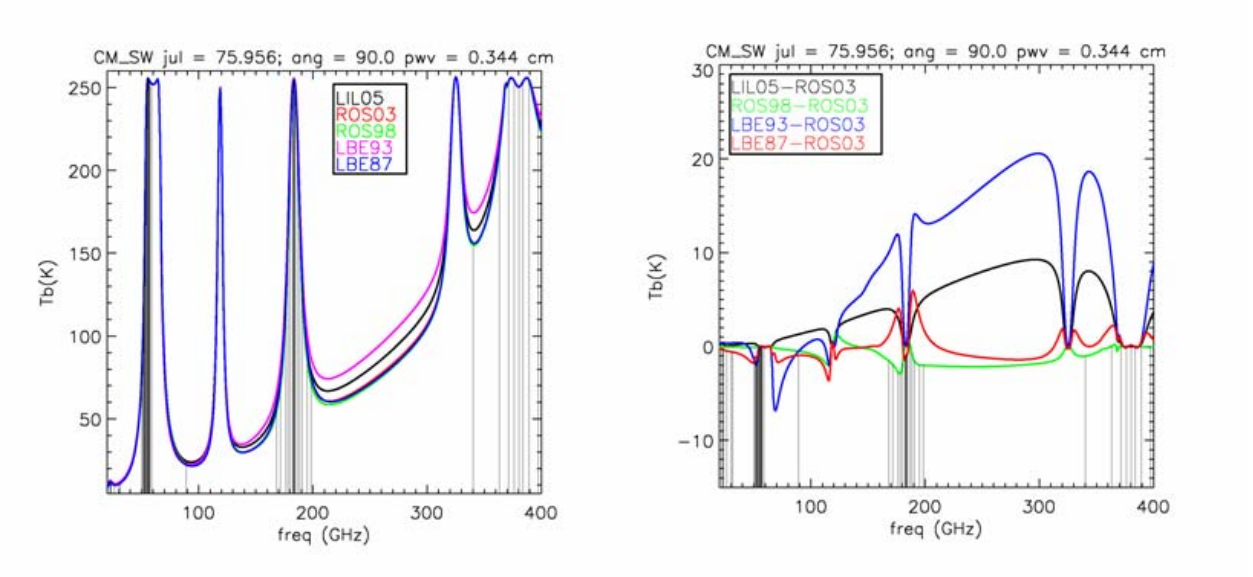

Figure 2. Comparison of forward model calculations for the Chilled Mirror radiosonde shown in Figure 1. Left-absolute values of Tb calculations. Right – differences in Tb calculations relative to the calculations of ROS03.

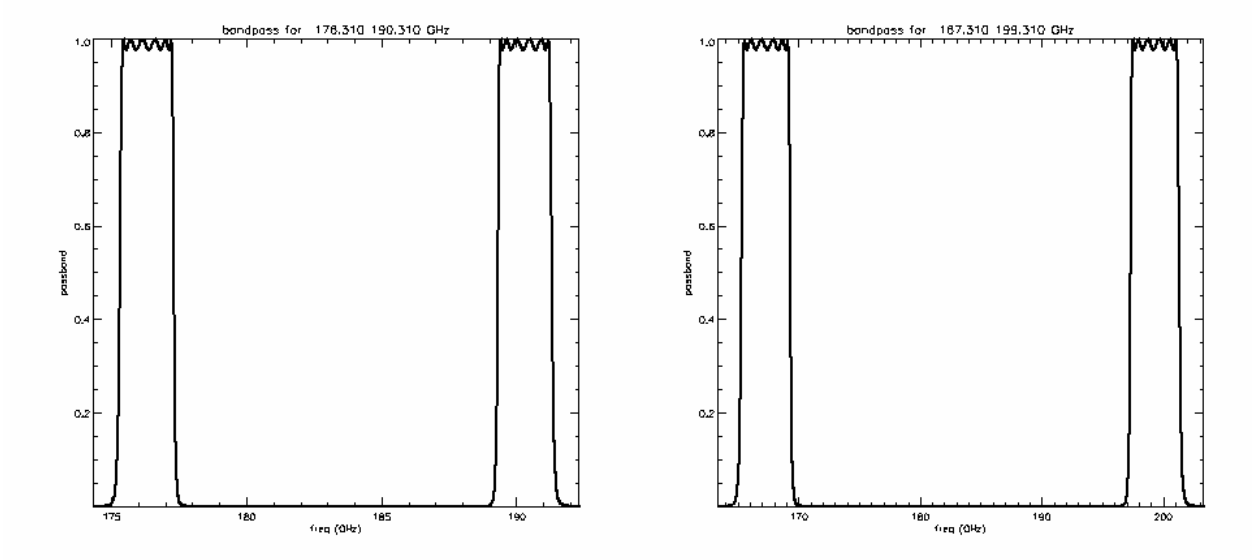

Figure 3. Examples of double-sided frequency filters for the GRS channels 183.31 ±7 and 183.31 ±16 GHz.

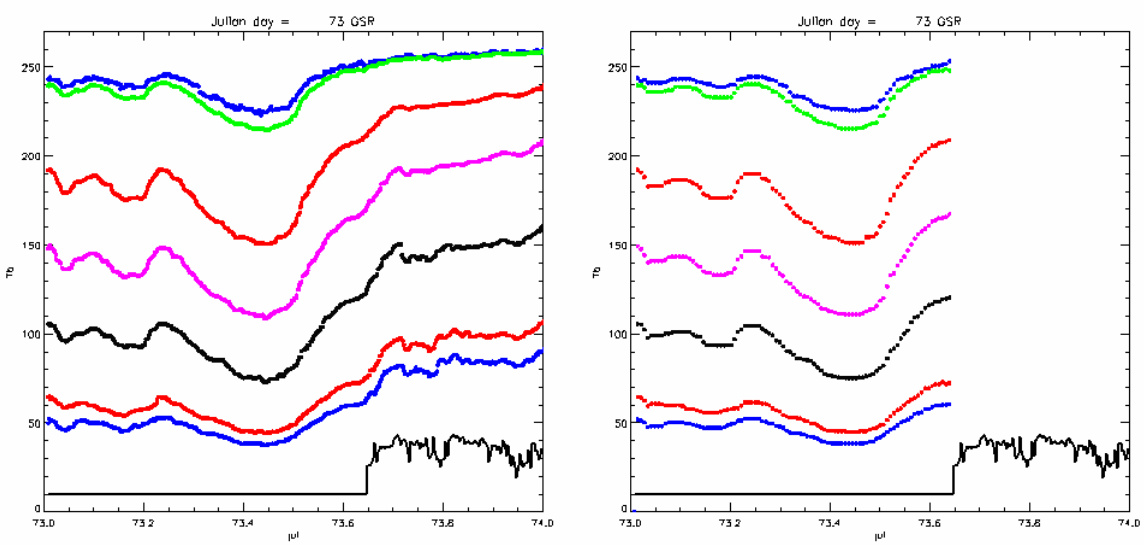

Figure 4. Left: GSR and MWRP data. Lower black curve is IR T_B from MWRP offset to 10 K from the clear condition value of 223.2 K. From bottom blue curve up, the GSR Channels are arranged in increasing order of frequency (183.31 + (±0.5, ±1, ±3, ±5, ±7, ±12,±16 GHz). Right: 10 min averages of GSR data during clear conditions. Cloud cleaning was achieved using IR T_B from the MWRP shown in the lower black curve.

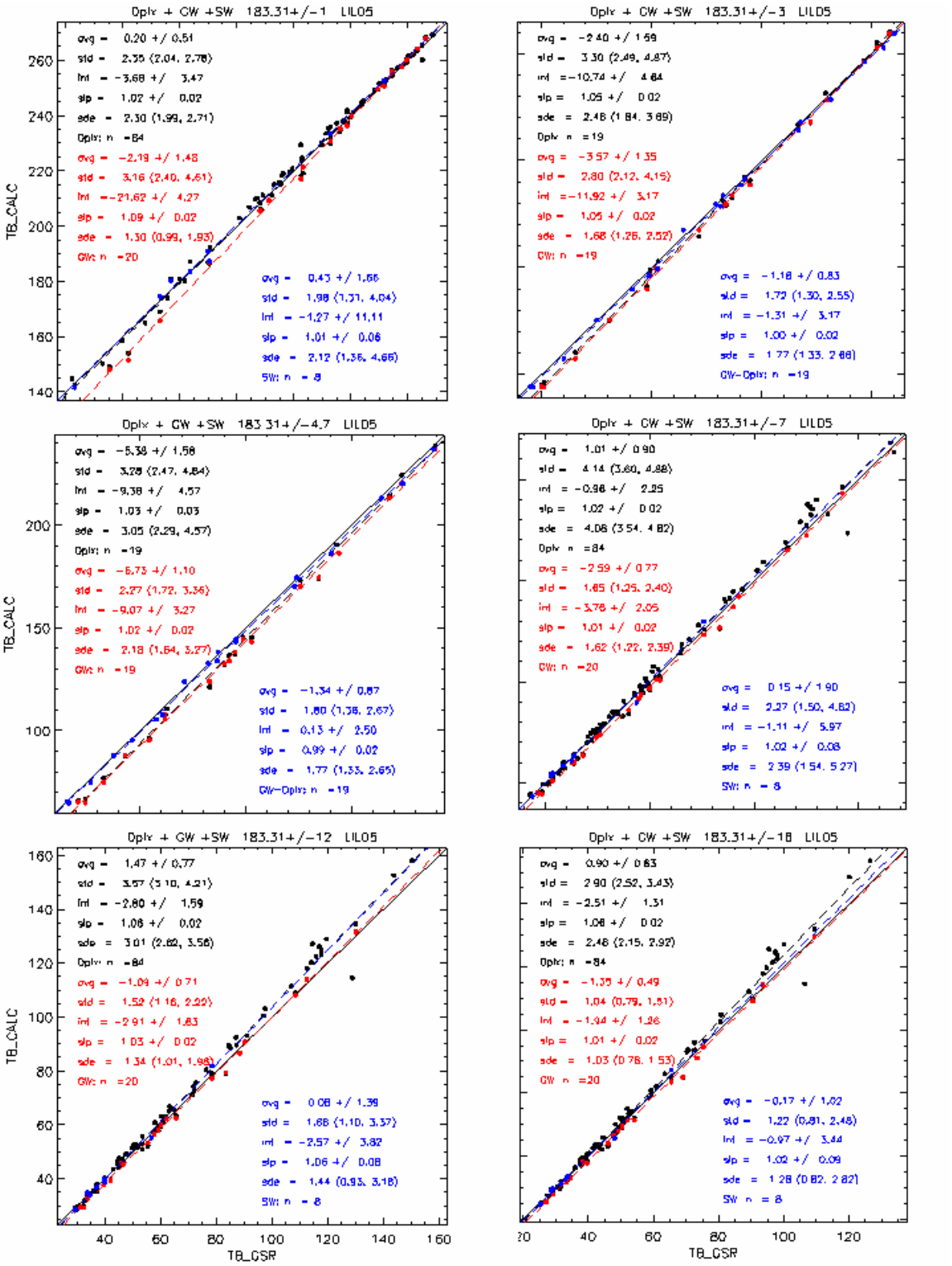

Figure 5. Comparisons of T_B model calculations with GSR measurements for the model of Liljegren et al. (2005). All comparisons refer to calculations minus measurements. The 95 % confidence intervals are also shown. Duplex (RS90) comparisons are in black, Great White (RS90) in red, and Duplex (Snow White) in blue.

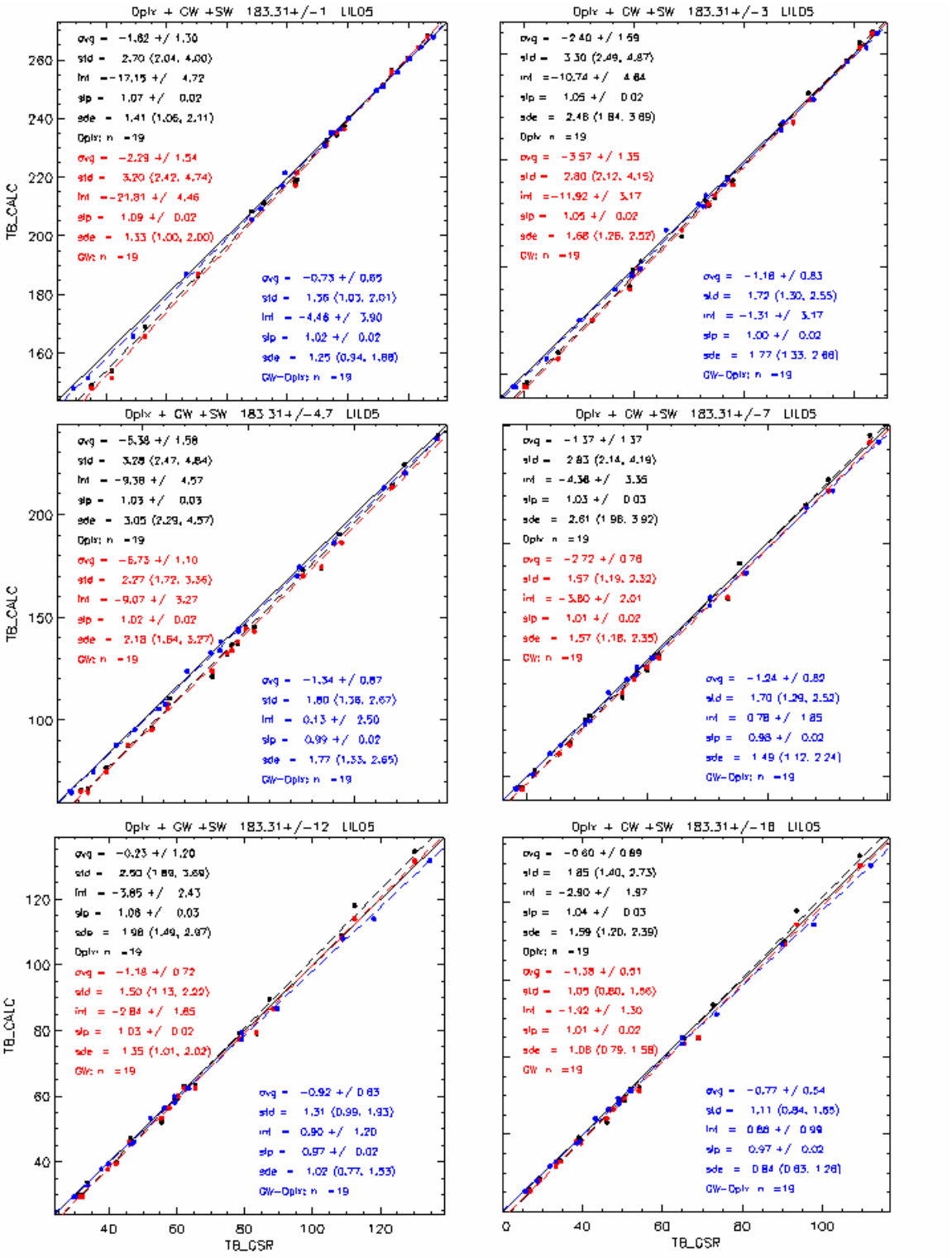

Figure 6. Comparisons of T_B model calculations with GSR measurements for the model of Liljegren et al. (2005) and for nearly simultaneous radiosonde launches at the Duplex and at the Great White.. All comparisons refer to calculations minus measurements. The 95 % confidence intervals are also shown. Duplex (RS90) comparisons are in black, Great White (RS90) in red, and statistics of the Great White minus the Duplex in blue.

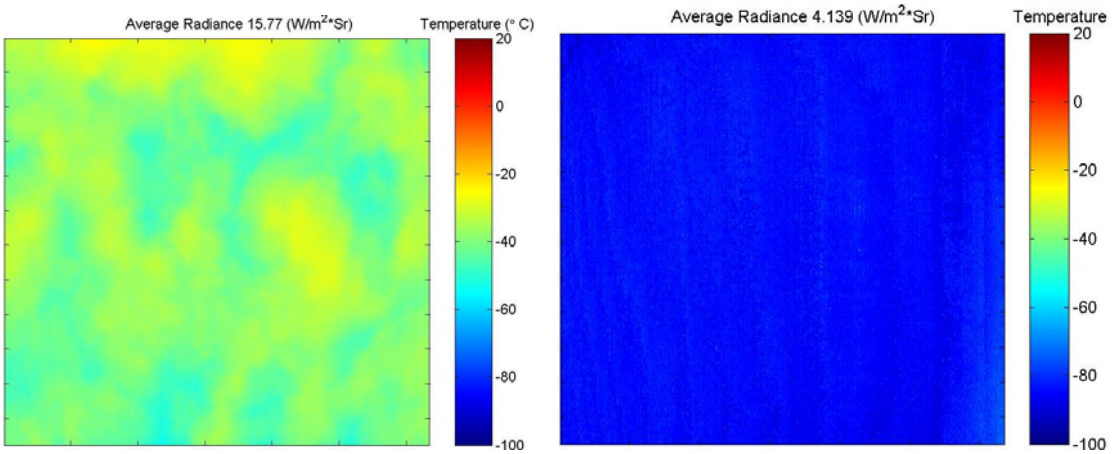

Figure 7. Infrared Cloud Imager (ICI) radiometric sky images showing (left) broken low clouds and (right) clear sky. The color bar indicates equivalent band-average brightness temperature in degrees C (ICI images are recorded in radiance, but displayed here in brightness temperature for convenience).